Formation and propagation of great salinity anomalies

H. Haak,[1] J. Jungclaus,[1] U. Mikolajewicz,[1] and M. Latif[2]

[1]   North Atlantic/Arctic ocean and sea ice variability for the period 1948–2001 is studied using a global Ocean General Circulation Model coupled to a dynamic/ thermodynamic sea ice model forced by daily NCEP/ NCAR reanalysis data [*Kalnay et al.*, 1996]. Variability of Arctic sea ice properties is analysed, in particular the formation and propagation of sea ice thickness anomalies that are communicated via Fram Strait into the North Atlantic. These export events led to the Great Salinity Anomalies (GSA) of the 1970s, 1980s and 1990s in the Labrador Sea (LS). All GSAs were found to be remotely excited in the Arctic, rather than by local atmospheric forcing over the LS. Sea ice and fresh water exports through the Canadian Archipelago (CAA) are found to be only of minor importance, except for the 1990s GSA. Part of the anomalies are tracked to the Newfoundland Basin, where they enter the North Atlantic Current. The experiments indicate only a minor impact of a single GSA event on the strength of the North Atlantic Thermohaline Circulation (THC).   INDEX TERMS: 4207 Oceanography: General: Arctic and Antarctic oceanography; 4255 Oceanography: General: Numerical modeling; 4215 Oceanography: General: Climate and interannual variability (3309); 4540 Oceanography: Physical: Ice mechanics and air/sea/ice exchange processes. **Citation:**   Haak, H., J. Jungclaus, U. Mikolajewicz, and M. Latif, Formation and propagation of great salinity anomalies, *Geophys. Res. Lett.*, *30*(9), 1473, doi:10.1029/2003GL017065, 2003.

1.   Introduction

[2]   The Arctic is an important fresh water source for the North Atlantic, influencing stratification and thus the vertical circulation in the North Atlantic sinking regions. Small variations in freshwater supply from the Arctic (via the East Greenland Current (EGC)) into the North Atlantic can alter or even prevent convection in the LS for several years. The GSA of the early 1970s [*Dickson et al.*, 1988] is an example of such an event. On the other hand, LS winter time deep convection is also influenced by the North Atlantic Oscillation (NAO) on interannual to decadal timescales [*Curry et al.*, 1998]. Previous modelling studies on this issues were based either on stand-alone sea ice models [*Hilmer et al.*, 1998], or limited domain coupled ocean/sea ice models [*Häkkinen*, 1999, *Köberle and Gerdes*, 2003]. Here a global ocean/sea ice model is used to investigate the North Atlantic/Arctic interactions and their impact on the THC. In particular, the chain of processes that led to GSAs in the

LS is presented self-consistently within the framework of a global ocean/sea ice model.

2.   Numerical Experiments

[3]   The Max-Planck-Institute ocean model (MPI-OM) is a primitive equation model (z-level, free surface), with the hydrostatic and Boussinesq assumptions made. MPI-OM includes an embedded dynamic/thermodynamic sea ice model with viscous-plastic rheology following *Hibler* [1979]. For details, see *Marsland et al.* [2003]. The particular model configuration has 40 vertical levels, with 20 of them in the upper 600 m. The horizontal resolution gradually varies between a minimum of 20 km in the Arctic and a maximum of about 350 km in the Tropics. The model is initialized from *Levitus et al.* [1998] climatological temperature and salinity data and integrated 11 times for the period 1948–2001 using daily NCEP/NCAR reanalysis forcing. On a global average NCEP/NCAR downward short wave radiation (DSWR) is appr. 10% higher than ERBE estimates or ECMWF reanalysis data. A global scaling factor of 0.89 is applied on DSWR to correct for this systematic bias in the forcing. In ice-free regions salinity in the surface layer (0–12 m) is restored towards the Levitus climatology, with a time constant of 180 days. The second and all subsequent integrations use the conditions at the end of the previous run as initial condition. The first two cycles are neglected in the following analysis to account for the models spinnup. To explore the response of the ocean/sea ice system to low-frequency fluctuations in the atmospheric forcing fields, additional sensitivity experiments were conducted. In these, a high pass (hp) filter is applied to certain forcing fields. The hp-filter removes climate variability with timescales longer than one month and maintains daily fluctuations and the climatological seasonal cycle. The sensitivity experiments are (1) all forcing fields hp-filtered (HPF ALL), (2) only wind stress hp-filtered (HPF TAU) and (3) all forcing fields except wind stress hp-filtered (HPF Q + FW).

3.   Results

[4]   Figure 1 shows the ensemble mean time evolution of Arctic sea ice volume. The time series exhibit pronounced interannual to multidecadal variability with distinct maxima in the mid 1960s, early 1980s and late 1980s. Sea ice volume increases from appr. 20000 km^3 in 1948 by almost 37% to 27500 km^3 in 1966. The ice covered area (not shown) increases at the same time by roughly 8% from 8.9 ∗ 10^6 km^2 to 9.6 ∗ 10^6 km^2, while the area-averaged Arctic sea ice thickness (not shown) increases by over 30% from 2.2 m to almost 2.9 m. Sea ice thickness stays at rather high values for the mid 1960s to mid 1980s. During the last 15 years of the simulation ice volume drops by appr. 30% from 28000 to 20000 km^3, ice area by 6% from 9.6 to 9.0 ∗ 10^6 km^2 and

[1]Max-Planck-Institut fuer Meteorologie, Hamburg, Germany.
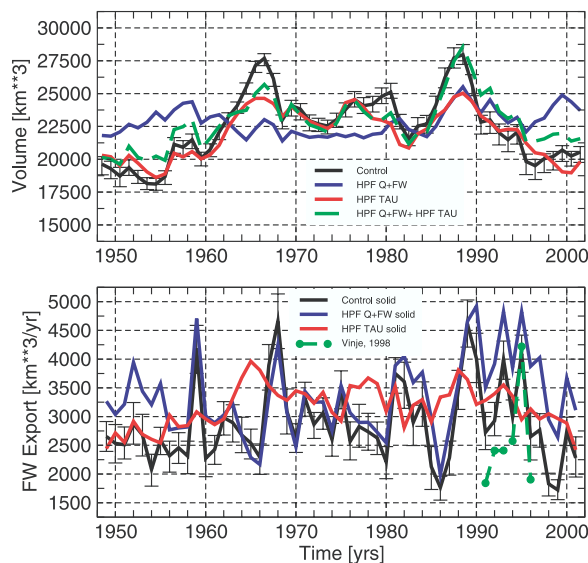[2]Institut fuer Meereskunde an der Universität Kiel, Germany.

Figure 1. Upper panel shows Arctic sea ice volume (excl. CAA) of control run (ensemble mean, bars indicate ensemble range; solid black) and runs HPF Q + FW (solid blue) and HPF TAU (solid red) and their linear super-position (dashed green). Units are km³. Lower panel shows Fram Strait freshwater export by sea ice and snow from control run (solid black) and from runs HPF Q + FW (blue) and HPF TAU (red) and observational estimates by *Vinje et al.* [1998]. Units are km³/yr.

sea ice thickness by 20% from 2.9 m to 2.3 m (not shown). The sensititivity experiments reveal that the Arctic sea ice volume variability is forced in equal parts by the wind and by thermal + freshwater forcing, respectively. A linear superposition of the sensitivity runs with hp-filtered wind stress and hp-filtered thermal + freshwater forcing reproduces the variability of the control run reasonably well. Arctic sea ice volume variability is mainly caused by sea ice thickness changes, and can be understood as a passive response to the atmospheric bondary conditions. Finally, no obvious long-term trend in Arctic sea ice volume can be seen in the simulation.

[5] Fram Strait sea ice exports are also shown in Figure 1. All volume transports are given in units of liquid freshwater. The time-mean freshwater transport by solid sea ice and snow, and its standard deviation with respect to annual values, amounts to 2874 ± 674 km³/yr. The liquid freshwater transport in Fram Strait (calculated with respect to the simulated climatological mean reference salinity of 35.0) is 1597 ± 397 km³/yr, with typical anomalies in the order of 600 to 700 km³/yr. Fram Strait sea ice export in our simulation is consistent with observational estimates of 2790 km³/yr by *Aagaard and Carmack* [1989] and 2565 ± 600 km³/yr for the 1990s by *Vinje et al.* [1998] and *Vinje* [2001]. Uncertainty is appr. 15% for the latter. The simulated variability of the volume transport agrees well with numerical experiments by *Hilmer et al.* [1998], *Köberle and Gerdes* [2003] and results presented in *Dickson et al.* [1999]. Fram Strait sea ice export is highly variable with individual anomalies reaching more than 60% of the mean value e.g., the maxima in winter 1967/68 (4658 km³/yr) and 1988/89 (4557 km³/yr). A few weaker peaks occur in 1958/59,

1980/81, 1992/93 and 1994/95. All peaks in ice export correspond, with a lag of about two years, to decreases in the Arctic sea ice volume, indicating at least parts of the the ice volume drops are caused by anomalous Fram Strait export events. The sensitivity experiment HPF Q + FW show clearly that the sea ice export is primarily driven by low-frequency variability in the wind forcing throughout the analysed period (Figure 1). Average exports through the CAA via Lancaster Sound (391 ± 134 km³/yr) as well as from Hudson Bay (205 ± 68 km³/yr) are both smaller than one standard deviation of the Fram Strait transports. Anomalous CAA fresh water (liquid + solid) export events are negative during the late 1960s and early 1980s. However, for the late 1980s the CAA export anomaly is positive and amounts to appr. 50% of the corresponding Denmark Strait value.

[6] Figure 2 illustrates the formation and propagation of the mid 1960s sea ice thickness anomaly that lead to the large Fram Strait sea ice export event of 1967/68. Anomalous winds led to an anomalous convergence of sea ice transports in the Laptev Sea in 1965/66. This convergence forms an
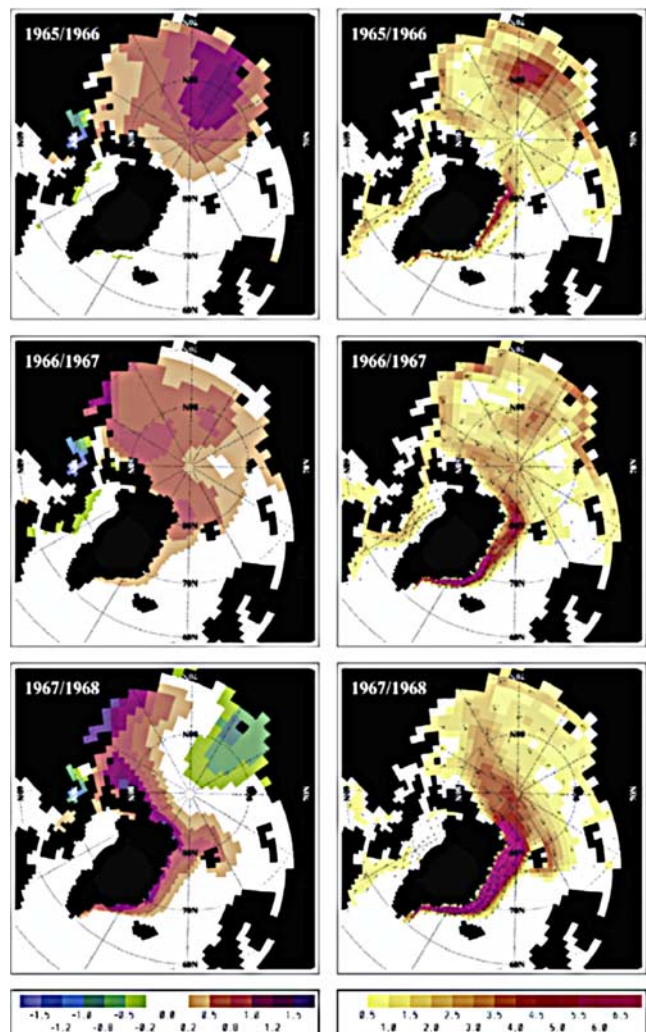

Figure 2. Ensemble mean sea ice thickness anomaly (left column) and sea ice transport anomaly (right column, every forth vector plotted) for the years 1965/66, 1966/67 and 1967/68. Shown are annual mean values centered on winter. Units are m and 10^{-2} m²/s, respectively.
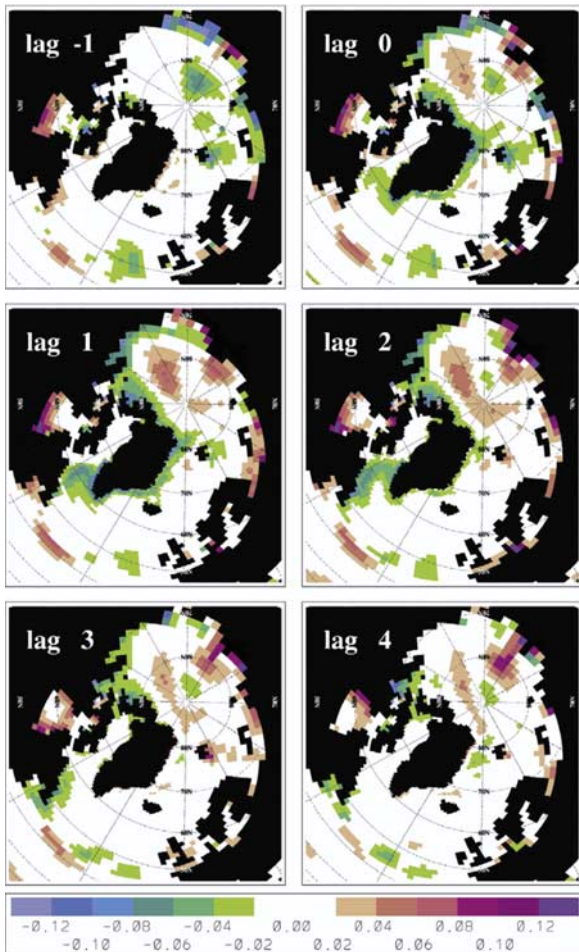
Figure 3. Regression of annual mean Fram Strait sea ice export on annual mean upper ocean $(0-335$ m) salinity anomaly (incl. sea ice and snow) from the control run for different time lags (integer years). Units are δS per one standard deviation of Fram Strait sea ice export.

initial sea ice thickness anomaly of about 1m. The anomaly propagates during the following year across the North Pole into the Canadian Sector and flushes in winter 1967/68 via Fram Strait into the Nordic Seas. The export event is accompanied by a weaker liquid freshwater anomaly of about 400 km^3/yr in the early to mid 1970s (not shown).

[7] Sea ice export events immediately influence upper ocean salinity in the EGC. Figure 3 shows a lag regression of Fram Strait sea ice export onto the salinity anomaly of the upper ocean $(0-335$ m). Note that most export events last for two following winters, resulting in lag 0 in our regression analysis based on annual, winter-centered (Aug.–Jul.) values. The regression reveals that average EGC salinity decreases shortly after the ice export event by an amplitude of about -0.1 per standard deviation of Fram Strait sea ice transport. For the 1967/68 export event the salinity decrease in the EGC locally exceeds -0.25. The low saline water is advected southward around Greenland into the LS. One part of the anomaly recirculates in the subpolar gyre, while another part enters Newfoundland Basin $3-4$ years after the peak in the export event. These anomalies enter the North Atlantic Current and follow the general circulation

eastward. However, they vanish before reaching the European Basin. Figure 4 shows the area-averaged ensemble mean near surface salinity in the central LS and the corresponding observations from Ocean Weather Ship (OWS) Bravo. The salinity decreases shortly after the export event, from 34.7 to 34.3 within the following three years. It reaches its minimum in 1971 and recovers afterwards. Around 1974 LS near surface salinity reaches 34.5 again. In both the simulations and the observations, LS deep convection reoccurs in winter 1971 and in the following years. The onset of LS deep convection is accompanied by above normal LS sea ice conditions in Davis Strait. The sensitivity experiments reveal, that severe atmospheric winter conditions over the LS, in particular the thermal + freshwater forcing during positive NAO phases, are driving the deep convection and the sea ice cover anomalies on interannual timescale (not shown). The model satisfactorily simulates the observed GSA which occured around 1970 in the LS (*Dickson et al.* [1988], *Lazier* [1995], *Belkin et al.* [1998]). Two additional GSAs are simulated, around 1980 and around 1990, in agreement with *Belkin et al.* [1998] and *Häkkinen* [2002]. The sensitivity runs reveal that low-frequency variations in the wind stress are sufficient to produce the 1970s GSA of appr. correct size. However, the low surface salinities on the LS persists for a longer time. The complementary run with the hp-filtered wind stress lacks the export event, and therefore also the GSA. The introduction of an artificial sea ice/fresh water anomaly of 3000 km^3 in 1967/68 into Fram Strait in a climatological forced run (HPF ALL), led to a slightly weaker GSA as in the control run (not shown).
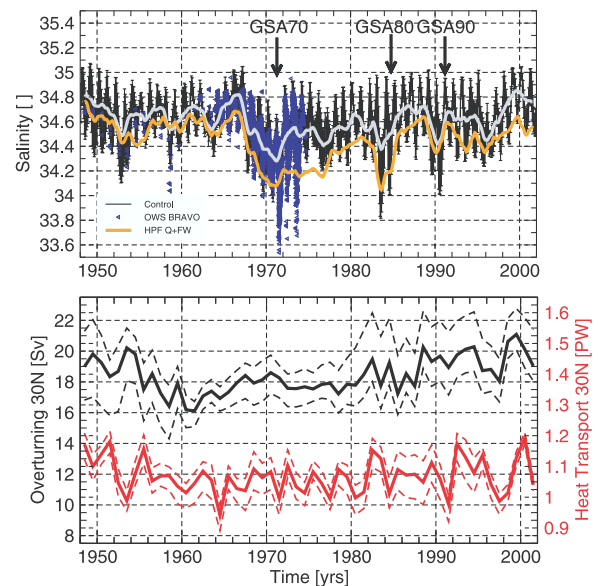

Figure 4. Upper panel shows Labrador Sea near surface salinity $(20-60$ m) from control run as monthly mean (ensemble mean, bars indicate ensemble range; black) and smoothed by a 12 month running mean (gray), sensitivity run HPF Q + FW (orange) and observations from OWS BRAVO (blue triangles). Lower panel shows Atlantic meridional overturning at $30°$N (black) and heat transport (red). Thin dashed lines indicate ensemble range. Units are Sv $(=10^6$ m^3/s) and PW respectively.

[8] Figure 4 also shows the strength of the Atlantic THC and the associated heat transport at 30°N. The time-mean overturning at 30°N and it's standard deviation with respect to annual mean values amounts to 18.4 ± 1.15 Sv ($=10^6\,m^3/s$), with pronounced interannual to decadal variability. The Atlantic heat transport at 30°N amounts to 1.01 ± 0.06PW. To assess the impact on the Atlantic THC, the runs HPF ALL with and without artificial GSA are compared. The Atlantic THC is barely affected by the introduction of the sea ice/freshwater anomaly. The difference in volume and heat transport is less than 0.3 Sv (0.05 PW) at 30°N and lasts only for a few years (not shown). The impact of the 1970s GSA seems to be slightly larger in the control run (Figure 4).

4. Discussion

[9] Our model is able to reproduce the chain of processes that led to the formation and propagation of Labrador Sea GSAs observed in the 1970s, 1980s 1990s. All GSAs are remotely driven by above normal freshwater exports via Fram Strait, that have their origin in anomalous Arctic sea ice properties. Anomalous winds lead to a convergence of sea ice transports in the Laptev sea. The resulting positive sea ice thickness anomaly is propagated across the North Pole and communicated via Fram Strait into the North Atlantic. Fram Strait ice export variability is primarily forced by low-frequency variations in the winds. Once a sea ice anomaly of appropriate size enters Fram Strait, a GSA will occur in the LS, consistently with previous results of *Häkkinen* [1999] for an idealized GSA. The simulated sea ice exports through the CAA and the local freshwater forcing have only minor importance in exciting GSAs, with the exception of the GSA90.

[10] However, the models horizontal resolution does not allow a proper representation of the CAA through-flow, and so some caution is advised in considering the former result. There is the possibility of local amplification of the remotely advected low salinity anomalies, once the winter-time deep convection in the LS is weakened or even shut-down, as discussed in *Houghton and Visbeck* [2002]. Vertical mixing by wintertime deep convection and hence the local atmospheric forcing over the LS plays an important role in removing the low surface salinities again. In particular, the NAO is driving central LS deep convection and Davis Strait sea ice conditions. As such, our simulations are consistent with the results of *Curry et al.* [1998] and *Deser et al.* [2002]. Each salinity anomaly can be tracked to the Newfoundland Basin. The simulated anomalies enter the North Atlantic Current, but vanish before reaching the European Basin, contrary to the observations by *Dickson et al.* [1988]. The life time of the anomalies in the simulation is probably underestimated due to strong mixing at the subpolar frontal system and the spurious damping effect of the surface salinity relaxation.

[11] Finally, the simulation reveals no strong impact of a single export event on the strength of the North Atlantic THC, contrary to the results of *Häkkinen* [1999]. The LS sinking region is affected only for a few years by the low salinities. An impact on the North Atlantic THC would largely depend on the frequency at which these export events occur, as well as the recovery time of the surface salinity, which is strongly influenced by the local atmospheric forcing.

References

Aagaard, K., and E. C. Carmack, The role of sea ice and other fresh water in the Arctic circulation, *J. Geophys. Res.*, 94, 14,485–14,498, 1989.

Belkin, I. M., S. Levitus, J. Antonov, and S.-A. Malmberg, Great Salinity Anomalies in the North Atlantic, *Prog. Oceanogr.*, 41, 1–68, 1998.

Curry, R. G., M. S. McCartney, and T. M. Joyce, Oceanic transport of subpolar climate signals to mid-depth subtropical waters, *Nature*, 391, 575–577, 1998.

Deser, C., M. Holland, G. Reverdin, and M. Timlin, Decadal variations in the Labrador Sea ice cover and North Atlantic sea surface temperatures, *J. Geophys. Res.*, 107(C5), art. no. 3035, 2002.

Dickson, R. R., J. Meincke, S.-A. Malmberg, and A. J. Lee, The Great Salinity Anomaly in the North Atlantic, *Nature*, 256(5517), 479–482, 1988.

Dickson, R. R., T. J. Osborn, J. W. Hurrel, J. Meincke, J. Blindheim, B. Adlandsvik, T. Vinje, G. Alekseev, and W. Maslowski, The Artic Ocean Response to the Nort Atlantic Oscillation, *J. Climate*, 13, 2671–2696, 1999.

Häkkinen, S., A Simulation of Thermohaline Effects of a Great Saliniy Anomaly, *Jornal of Climate*, 12, 1781–1795, 1999.

Häkkinen, S., Freshning of the Labrador Sea surface water in the 1990s: Another Great Salinity Anomaly?, *Geophys. Res. Let.*, 29(24), 2232–2235, 1990.

Hibler, W. D., A dynamic thermodynamic sea ice model, *J. Phys. Oceanogr.*, 9, 815–846, 1979.

Hilmer, M., M. Harder, and P. Lemke, Sea ice transport: a highly variable linkbetween Arctic and North Atlantic, *Geophys. Res. Let.*, 25(17), 3359–3362, 1998.

Houghton, R. W., and M. Visbeck, Quasi-decadal salinity fluctuations in the Labrador Sea, *J. Phys. Oceanogr.*, 32, 687–701, 2002.

Kalnay, E., et al., The NCEP/NCAR 40-Year reanalysis project, *Bull. Amer. Meteor. Soc.*, 77(3), 437–470, 1996.

Köberle, C., and R. Gerdes, Mechanisms determining the variability of Arctic sea ice conditions and export, *Journal of Climate*, accepted, 2003.

Lazier, J. R. N., The salinity decrease in the Labrador Sea over the last 30 years, *Natural Climate Variability on Decade to Century Timescales*, edited by D. G. Martinson et al., National Academic Press, 295–302, 1995.

Levitus, S., T. B. Boyer, M. E. Conkright, T. O'Brian, J. Antonov, C. Stephens, L. Stathoplos, D. Johnson, and R. Gelfeld, World Ocean Database 1998, Volume 1, Introduction, NOAA Atlas NESDIS18, Ocean Climate Laboratory, National Oceanographic Data Center, U.S. Gov. Printing Office, Wash., D. C., 1998.

Marsland, S. J., H. Haak, J. H. Jungclaus, M. Latif, and F. Roeske, The Max-Planck-Institute global ocean/sea ice model with orthogonal curvi-linear coordinates, *Ocean Modelling*, 5(2), 91–127, 2003.

Vinje, T. N., N. Nordlund, and A. Kvambek, Monitoring ice thickness in Fram Strait, *J. Geopys. Res.*, 103, 10,437–10,449, 1998.

Vinje, T., Strait Ice Fluxes and Atmospheric Circulation: 1950–2000, *Journal of Climate*, 14, 3508–3517, 2001.

————————————

H. Haak, J. Jungclaus, and U. Mikolajewicz, Max-Planck-Institut fuer Meteorologie, Bundesstr. 55, 20148 Hamburg, Germany. (haak@dkrz.de)

M. Latif, Institut fuer Meereskunde an der Universität Kiel, Germany.